N^4C−Ethyl−N^4C Cross-Linked DNA: Synthesis and Characterization of Duplexes with Interstrand Cross-Links of Different Orientations†

Anne M. Noronha,‡ David M. Noll,§ Christopher J. Wilds,|| and Paul S. Miller*,‡

Department of Biochemistry and Molecular Biology, Bloomberg School of Public Health, Johns Hopkins University, 615 North Wolfe Street, Baltimore, Maryland 21205, Department of Biophysics and Biophysical Chemistry, School of Medicine, Johns Hopkins University, 725 North Wolfe Street, Baltimore, Maryland 21205, and Department of Biological Sciences, Vanderbilt University, 2326 Stevenson Center, Nashville, Tennessee 37232

Received August 6, 2001; Revised Manuscript Received November 13, 2001

ABSTRACT: The preparation and physical properties of short DNA duplexes that contain a N^4C−ethyl−N^4C interstrand cross-link are described. Duplexes that contain an interstrand cross-link between mismatched C−C residues and duplexes in which the C residues of a −CG− or −GC− step are linked to give "staggered" interstrand cross-links were prepared using a novel N^4C−ethyl−N^4C phosphoramidite reagent. Duplexes with the C−C mismatch cross-link have UV thermal transition temperatures that are 25 °C higher than the melting temperatures of control duplexes in which the cross-link is replaced with a G−C base pair. It appears that this cross-link stabilizes adjacent base pairs and does not perturb the structure of the helix, a conclusion that is supported by the CD spectrum of this duplex and by molecular models. An even higher level of stabilization, 49 °C, is seen with the duplex that contains a −CG− staggered cross-link. Molecular models suggest that this cross-link may induce propeller twisting in the cross-linked base pairs, and the CD spectrum of this duplex exhibits an unusual negative band at 298 nm, although the remainder of the spectrum is similar to that of B-form DNA. Mismatched C−C or −CG− staggered cross-linked duplexes that have complementary overhanging ends can undergo self-ligation catalyzed by T4 DNA ligase. Analysis of the ligated oligomers by nondenaturing polyacrylamide gel electrophoresis shows that the resulting oligomers migrate in a manner similar to that of a mixture of non-cross-linked control oligomers and suggests that these cross-links do not result in significant bending of the helix. However, the orientation of the staggered cross-link can have a significant effect on the structure and stability of the cross-linked duplex. Thus, the thermal stability of the duplex that contains a −GC− staggered cross-link is 10 °C lower than the melting temperature of the control, non-cross-linked duplex. Unlike the −CG− staggered cross-link, in which the cross-linked base pairs can still maintain hydrogen bond contacts, molecular models suggest that formation of the −GC− staggered cross-link disrupts hydrogen bonding and may also perturb adjacent base pairs leading to an overall reduction in helix stability. Duplexes with specifically positioned and oriented cross-links can be used as substrates to study DNA repair mechanisms.

A variety of environmental and therapeutic agents react with DNA to produce interstrand cross-links. These lesions, which prevent DNA strand separation during transcription or replication, are potentially lethal to the cell (*1*−*3*) and are considered to be therapeutically important lesions in cancer chemotherapy (*4*). Cells have evolved methods of repairing or otherwise circumventing these lesions (*5*). Although a number of repair pathways, including homologous recombination and nucleotide excision repair, have been implicated in cross-link repair in bacteria, yeast, and mammalian cells, a clear understanding of the molecular mechanisms that are involved is still lacking. Such understanding could be of considerable importance in designing effective therapeutic agents whose mode of action depends on interstrand cross-link formation.

Mechanistic studies of repair processes both in vitro and in cells would be facilitated significantly by the availability of substrates of defined chemical structure. One way to prepare such substrates involves reaction of a DNA duplex with a cross-linking agent. Thus, for example, oligodeoxyribonucleotide duplexes with a −GNC− sequence react with bifunctional alkylating agents such as nitrogen mustards to give duplexes containing N^7G-alkyl-N^7G interstrand cross-links (*6*−*9*). This general approach has been used to prepare duplexes that contain a variety of interstrand cross-links, including those from reaction with psoralen derivatives (*10*), platinum compounds (*11*, *12*), mitomycin C (*13*, *14*), nitrous acid (*15*), formaldehyde (*16*), 2,5-bis(1-aziridinyl)-1,6-benzoquinone (*17*), bifunctional pyrroles (*18*), *N*,*N*′-bis(2-

† This research was supported by a grant from the National Cancer Institute (CA082785). A.M.N. and C.J.W. were each supported in part by postdoctoral fellowships from the Natural Sciences and Engineering Research Council of Canada (NSERC). D.M.N. was supported by grants from the Robert Leet and Clara Guthrie Patterson Trust and The Alexander and Margaret Stewart Trust.

* To whom correspondence should be addressed. Phone: (410) 955-3489. Fax: (410) 955-2926. E-mail: pmiller@jhsph.edu.

‡ Bloomberg School of Public Health, Johns Hopkins University.

§ School of Medicine, Johns Hopkins University.

|| Vanderbilt University.

10.1021/bi011610u CCC: $22.00 © 2002 American Chemical Society
Published on Web 12/22/2001

chloroethyl)nitrosourea (BCNU) (*19*), and malondialdehyde (*20*). Drawbacks of this approach include low reaction yield and the potential generation of multiple side products such as monoadducts which complicate purification of the cross-linked duplex.

A more direct approach involves de novo synthesis of the cross-linked duplex on an automated DNA synthesizer. The cross-link is first introduced during the synthesis of one strand of the oligonucleotide duplex, creating a branch point at the 5′-end of the oligomer. Selective deprotection and chain extension then allows synthesis of the complete cross-linked duplex. This approach was first used to prepare an oligodeoxyribonucleotide duplex containing a N^2G-N^2G nitrous acid cross-link (*21*).

We recently described the de novo syntheses of short DNA duplexes that contain an $N^4C-ethyl-N^4C$ interstrand cross-link (*22*). This C−C cross-link mimics the BCNU-generated G−C cross-link and a recently described C−C mismatch cross-link found in DNA that was treated with mechloroethamine, a bifunctional alkylating agent (*23*, *24*). A convertible nucleoside approach was used to introduce the cross-link during automated synthesis of the cross-linked duplex.

In this paper, we describe an alternative approach to synthesizing $N^4C-ethyl-N^4C$ interstrand cross-linked duplexes which employs a $N^4C-ethyl-N^4C$ phosphoramidite reagent. We have used this reagent to prepare a number of novel cross-linked duplexes, including duplexes that contain an interstrand cross-link between two mismatched C−C residues and duplexes in which the C residues of a −CG− or −GC− step are linked to give "staggered" interstrand cross-links. In addition to their syntheses and characterization, we describe some of the physical properties of these cross-linked duplexes.

EXPERIMENTAL PROCEDURES

5′-*O*-(Dimethoxytrityl)-2′-deoxyuridine (**1.1**), 5′-*O*-(dimethoxytrityl)-3′-*O*-(*tert*-butyldimethylsilyl)-2′-deoxyuridine (**1.2**), and 5′-*O*-(dimethoxytrityl)-3′-*O*-(*tert*-butyldimethylsilyl)-4-(*N*-1-triazolyl)-2′-deoxyuridine (**1.3**) were prepared as previously described (*22*). 5′-*O*-(Dimethoxytrityl)deoxyribonucleoside-3′-*O*-(β-cyanoethyl-*N*,*N*′-diisopropyl)phosphoramidites, 3′-*O*-(dimethoxytrityl)deoxyribonucleoside-5′-*O*-(β-cyanoethyl-*N*,*N*′-diisopropyl)phosphoramidites, and protected deoxyribonucleoside-controlled pore glass supports were purchased from Glen Research (Sterling, VA) and ChemGenes (Ashland, MA). Strong anion exchange (SAX) HPLC was carried out using a Dionex DNAPAC PA-100 column (0.4 cm × 25 cm) purchased from Dionex (Sunnyvale, CA). Reversed phase HPLC was carried out using a Microsorb C-18 column (0.46 cm × 15 cm) purchased from Varian Associates (Walnut Creek, CA).

The SAX column was eluted with a 30 mL linear gradient of sodium chloride in a buffer that contained 100 mM Tris (pH 7.8) in 10% acetonitrile at a flow rate of 1.0 mL/min. The C-18 column was eluted with a 20 mL linear gradient of acetonitrile in 50 mM phosphate buffer (pH 5.8) at a flow rate of 1.0 mL/min. The columns were monitored at 260 nm for analytical runs or 290 nm for preparative runs. Denaturing polyacrylamide gel electrophoresis was carried out on 20 cm × 20 cm × 0.75 cm gels containing 20% acrylamide and 7 M urea in TBE which contained 89 mM Tris, 89 mM boric acid, and 0.2 mM ethylenediaminetetraacetate buffered at pH 8.0. Native polyacrylamide gel electrophoresis was carried out on 20 cm × 20 cm × 0.75 or 20 cm × 40 cm × 0.75 cm gels containing 12 or 20% polyacrylamide in TBE. The running buffer was TBE. ^{32}P-labeled oligonucleotides were detected by autoradiography or by phosphorimaging. Mass spectra were obtained at the John Hopkins University School of Medicine Mass Spectrometry Facility or at the Scripps Research Institute Mass Spectrometry Facility.

*5′-O-(Dimethoxytrityl)-3′-O-(trimethylsilyl)-2′-deoxyuridine (**1.4**)*. To a suspension of the nucleoside **1.1** (4.0 g, 7.52 mmol) in methylene chloride (75 mL) were added triethylamine (5 mL, 35.3 mmol, 4.7 equiv) and then trimethylsilyl chloride (2.38 mL, 18.8 mmol, 2.5 equiv), and the mixture was allowed to stir at room temperature for 1 h. The reaction was quenched by the addition of methanol (10 mL); the solution was stirred for an additional 10 min and then extracted with two portions (200 mL each) of saturated sodium bicarbonate followed by two portions (200 mL each) of saturated sodium chloride. The organic layer was dried over anhydrous magnesium sulfate and, following filtration, evaporated to yield a pink foam in quantitative yield. TLC: $R_f = 0.34$ (5:95 methanol/chloroform) and 0.50 (10:90 methanol/chloroform).

*5′-O-(Dimethoxytrityl)-3′-O-(trimethylsilyl)-4-(N-1-triazolyl)-2′-deoxyuridine (**1.5**)*. To a suspension of 1,2,4-triazole (8.01 g, 119 mmol, 16 equiv) in a dichloromethane/acetonitrile mixture (1:1, 120 mL) was added triethylamine (23 mL, 171 mmol, 23 equiv) and the mixture stirred at 0 °C for 5 min. Phosphorus oxychloride (1.7 mL, 18.6 mmol, 2.5 equiv) was added dropwise, and the solution became a thick white slurry. A solution of **1.4** (4.5 g, 7.46 mmol) in acetonitrile (20 mL) was added, and the reaction mixture turned pink immediately. After 40 min, the starting material was completely converted to the triazole intermediate **1.5** as evidenced by TLC. The reaction mixture was diluted with methylene chloride and worked up as in the case of **1.4** to yield the title compound **1.5** as a foam (4.57 g, 94%). TLC: $R_f = 0.17$ (3:2 toluene/ethyl acetate).

*5′-O-(Dimethoxytrityl)-N⁴-(2-aminoethyl)-2′-deoxycytidine (**1.6**)*. The crude nucleoside **1.5** (4.57 g, 7.08 mmol) was taken up in 1,4-dioxane (85 mL). Ethylenediamine was slowly added (19.7 mL, 304 mmol, 43 equiv). The solution turned bright yellow immediately, indicating the release of the triazole moiety. The reaction mixture was allowed to stir at room temperature for 1 h, and the solvent was removed under vacuum. Coevaporation with methanol followed by ether resulted in the loss of the trimethylsilyl (TMS) group to give one spot identified as the desired product. TLC: $R_f = 0.067$ (3:2 toluene/ethyl acetate) and 0.35 (8:2 methylene chloride/methanol). The crude gum was purified by column chromatography using a gradient of 0 to 2% methanol in methylene chloride containing 2% triethylamine to afford the desired product **1.6** as a light yellow foam (2.29 g, 54% yield).

*1-{N⁴-[5′-O-(Dimethoxytrityl)-3′-O-(tert-butyldimethylsilyl)-2′-deoxycytidylyl]}-2-{N⁴-[5′-O-(dimethoxytrityl)-2′-deoxycytidylyl]}ethane (**1.7**)*. To a solution of nucleoside **1.6** (1.08 g, 1.87 mmol) in pyridine (20 mL) was added triethylamine (1.5 mL, 10.6 mmol, 5.7 equiv), followed by nucleoside **1.3** (1.07 g, 1.55 mmol, 0.8 equiv). The reaction

Name	Sequence	Orientation
XL1	d-CGAAACTTTCG GCTTTCAAAGC-d	mismatched C-C
XL2	d-AAACTTTGGG CCCTTTCAAA-d	mismatched C-C
XL3	d-GAACGTTCGG CCCTTGCAAG-d	-CG- staggered
XL4	d-CCCCCCGAACGTTCGG GGCTTGCAAGCCCCCC-d	-CG- staggered
XL5	d-GAAGCTTCGG CCCTTCGAAG-d	-GC- staggered
XL6	d-CCCCCCGAAGCTTCGG GGCTTCGAAGCCCCCC-d	-GC- staggered

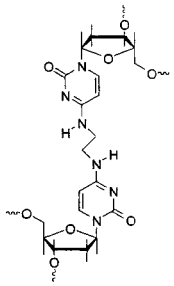

FIGURE 1: Sequences of the cross-linked duplexes. The 5′-end of each strand of the duplex is denoted by the symbol d-. The structure of the N^4C−ethyl−N^4C cross-link is shown at the right.

mixture was allowed to stir at room temperature overnight. The reaction was complete as judged by silica gel TLC [R_f = 0.26 (4.5:4.5:1 toluene/ethyl acetate/methanol)], and the solution was evaporated to dryness. Silica gel column chromatography of the reaction mixture using a gradient of 0 to 5% methanol in methylene chloride containing 2% triethylamine yielded 1.1 g (61%) of **1.7**. TLC: R_f = 0.24 (10:90 methanol/chloroform). EI-MS (matrix, NBA): calcd (M), 1199; found (MH^+), 1199.6. The protecting groups were removed by treating **1.7** with 80% aqueous acetic acid at 67 °C for 1 h. The retention time of the deprotected C−C cross-link (11 min) using a 0 to 50% acetonitrile gradient was identical to that of previously prepared C−C cross-link (*22*).

*1-{N^4-[5′-O-(Dimethoxytrityl)-3′-O-(tert-butyldimethylsilyl)-2′-deoxycytidyl]}-2-{N^4-[5′-O-(dimethoxytrityl)-2′-deoxycytidyl-3′-O-(β-cyanoethyl-N,N′-diisopropyl)-phosphoramidite]}ethane (**1.8**)*. To a solution of nucleoside **1.7** (0.51 g, 0.43 mmol) in dry methylene chloride (4 mL) was added *N*,*N*-diisopropylamine tetrazolide (0.123 g, 0.72 mmol, 1.7 equiv) followed by 2-cyano-*N*,*N*,*N*′,*N*′-tetraisopropylphosphorane (351 μL, 1.06 mmol, 2.5 equiv). The solution was stirred for 90 min at room temperature. The product was detected by silica gel TLC [R_f = 0.47 and 0.35 (5:90:5 methanol/ethyl acetate/triethylamine)]. Dry methylene chloride was added to stop the reaction, and the reaction mixture was worked up in the same manner as described for **1.4** to give a foam. The product was purified by silica gel column chromatography using a methanol/ethyl acetate/triethylamine gradient from 0, 99.5, and 0.5% to 3, 96.5, and 0.5% to yield 0.302 g of a white foam (50%). EI-MS (matrix, NBA): calcd (M), 1400; found (MH^+), 1399.8. ^{31}P NMR (acetone-d_6): δ 150.91, 150.69.

Syntheses of Cross-Linked Duplexes. The cross-linked duplexes, the sequences of which are shown in Figure 1, were assembled on an Applied Biosystems model 392A synthesizer using standard cyanoethyl phosphoramidite chemistry (*25*, *26*). Long chain alkylamine-controlled pore glass (CPG) was used as the solid support. The nucleoside phosphoramidites were prepared in anhydrous acetonitrile at a concentration of 0.15 M for the 3′-phosphoramidites or 0.3 M for the 5′-phosphoramidites. Assembly of sequences was carried out as follows: (a) detritylation, 2% dichloroacetic acid in dichloromethane delivered in four 10 s increments, each followed by a 10 s "wait" period, (visual observation of the trityl eluates gave condensation yields that were ≥90%); (b) nucleoside phosphoramidite coupling times of 2 min for commercial phosphoramidites and 10 min for the C−C cross-linked phosphoramidite; (c) capping, 1:1 (v/v) mixture of a 1:1:8 (v/v/v) acetic anhydride/collidine/tetrahydrofuran mixture (solution A) and a 16:84 (w/v) 1-methyl-1*H*-imidazole/tetrahydrofuran mixture (solution B) delivered in two 10 s increments each followed by a 10 s wait period; and (d) oxidation, 0.1 M iodine in a 2.5:2:1 tetrahydrofuran/water/pyridine mixture, delivered in an 8 s increment followed by a 15 s "wait". The cyanoethyl groups were removed from the CPG-linked oligomers by treating the support with 1 mL of anhydrous triethylamine (TEA) for at least 12 h. The support was washed with 30 mL of anhydrous acetonitrile followed by anhydrous tetrahydrofuran. The *tert*-butyldimethylsilyl group was removed from the partial duplex by treating the support with 1 mL of a 1.0 M solution of tetra-*n*-butylammonium fluoride in tetrahydrofuran (stored over molecular sieves) for 10 min (duplexes **XL2** and **XL3**) or 20 min (oligomer **XL1**). The support was then washed with 30 mL of anhydrous tetrahydrofuran and 30 mL of acetonitrile. The last segment of the duplex was then synthesized using 5′-phosphoramidites with a total detritylation exposure time of 120 s. The 3′-terminal trityl group was removed by the synthesizer.

The oligomer-derivatized CPG was transferred from the reaction column to autosampler vials fitted with Teflon-lined caps, and the protecting groups were removed by treatment with 0.4 mL of concentrated ammonium hydroxide for 6 h at 65 °C. The cross-linked duplexes were purified by SAX HPLC. The retention times of the duplexes are shown in Table 1. In the case of **XL2**, the peak was quite broad and the duplex was not pure. Consequently, the HPLC fractions containing duplex **XL2** were combined and further purified by preparative gel electrophoresis on a 20% denaturing gel. This additional purification resulted in the loss of material which accounts for the low yield of the duplex. The purified oligomers were desalted using C-18 SEP PAK cartridges (Waters Inc.) as previously described (*22*). The amounts of purified oligomers that were obtained are shown in Table 1.

The cross-linked oligomers (0.1 A_{260} unit) were characterized by digestion with a combination of snake venom phosphodiesterase (0.28 unit) and calf intestinal phosphatase (5 units) in a buffer containing 10 mM Tris (pH 8.1) and 2 mM magnesium chloride as previously described (*22*). The resulting mixture of nucleosides was analyzed by reversed phase HPLC and the ratio of nucleosides determined (*22*). The results are given in Table 1. The molecular weight of each cross-linked oligomer was determined by MALDI-TOF mass spectrometry, and the results are shown in Table 1.

UV Thermal Denaturation Studies. Molar extinction coefficients for the oligonucleotides and cross-linked duplexes were calculated from those of the mononucleotides and dinucleotides according to nearest-neighbor approximations (units = 10^4 M^{-1} cm^{-1}) (*27*). Non-cross-linked duplexes were prepared by mixing equimolar amounts of the interacting strands and lyophilizing the resulting mixture to dryness. The resulting pellet was then redissolved in 90 mM sodium chloride, 10 mM sodium phosphate, and 1 mM EDTA (pH 7.0) to give a final concentration of 1 μM in each strand. The cross-linked duplexes were dissolved in the same buffer to give a final concentration of 1 μM. The solutions were then heated to 65 °C for 15 min, cooled slowly to room

Table 1: Amounts, Retention Times, Nucleoside Ratios, and Mass Spectral Data for Cross-Linked Duplexes

cross-linked duplex	A_{260} units	retention time (min)[a]	nucleoside composition	nucleoside ratio		mass	
				expected	observed	expected	observed
XL1	34.18	25.71[b]	dC	4.00	3.85	6656	6661
			dG	2.00	2.13		
			dT	1.00	1.00		
			dA	1.00	1.06		
			dC-dC	1.00	1.00		
XL2	0.40	25.39[b]	dC	1.00	1.00	6039	6042
			dG	1.00	0.85		
			dT	2.00	2.09		
			dA	2.00	1.72		
			dC-dC	0.67	0.26		
XL3	31.0	26.45[b]	dC	4.00	4.07	6081	6085
			dG	6.00	5.77		
			dT	4.00	4.00		
			dA	4.00	3.68		
			dC-dC	1.00	1.00		
XL4	4.10	22.51[c]	dC	4.00	3.85	9628	9628
			dG	2.00	2.13		
			dT	1.00	1.00		
			dA	1.00	1.06		
			dC-dC	1.00	1.00		
XL5	26.00	25.91[b]	dC	1.00	1.00	6081	6077
			dG	1.50	1.48		
			dT	1.00	0.98		
			dA	1.00	1.00		
			dC-dC	0.50	0.42		
XL6	2.70	22.37[c]	dC	3.50	3.83	9628	9624
			dG	2.00	2.09		
			dT	1.00	1.00		
			dA	1.00	1.20		
			dC-dC	1.00	1.00		

[a] Strong anion exchange HPLC. [b] With 0.0−0.5 M sodium chloride in 0.1 M Tris (pH 7.8) and 10% acetonitrile. [c] With 0.0−0.7 M sodium chloride in 0.1 M Tris (pH 7.8) and 10% acetonitrile.

temperature, and stored at 4 °C overnight before measurements were taken. Prior to the thermal run, samples were degassed by placing them in a speed-vac concentrator for 2 min. Denaturation curves were acquired at 260 nm at a heating rate of 0.5 °C/min, using a Varian CARY model 3E spectrophotometer fitted with a six-sample thermostated cell block and a temperature controller. The data were analyzed in accordance with the convention of Puglisi and Tinoco (*27*) and transferred to Microsoft Excel.

Circular Dichroism Spectra and CD Spectroscopy. Circular dichroism spectra were obtained on a Jasco J-700 spectropolarimeter equipped with a NESLAB RTE-111 circulating bath. Samples were allowed to equilibrate for 5−10 min at 5 °C in 90 mM sodium chloride, 10 mM sodium phosphate, and 1 mM EDTA (pH 7.0), at a final concentration of 2 μM in each strand for the cross-linked duplexes and ca. 3.6 μM for control duplexes. Molar extinction coefficients for oligonucleotides were calculated from those of the mononucleotides and dinucleotides according to nearest-neighbor approximations (units = 10^4 M^{-1} cm^{-1}) as reported for the UV denaturation studies. Each spectrum was an average of five scans. Spectra were collected at a rate of 100 nm/min with a bandwidth of 1 nm and a sampling wavelength of 0.2 nm using fused quartz cells (Hellma, 165-QS). The CD spectra were recorded from 350 to 200 nm at 5 °C. The molar ellipticity was calculated from the equation $[\theta] = \theta/Cl$, where θ is the relative ellipticity (millidegrees), C is the molar concentration of oligonucleotides (moles per liter), and l is the path length of the cell (centimeters). The data were processed on a personal computer using Windows-based software supplied by the manufacturer (JASCO, Inc.) and transferred into Microsoft Excel for presentations.

Self-Ligation of Cross-Linked Duplexes and Gel Analysis. Cross-linked duplexes **XL2**, **XL3**, and **XL5** (0.21 nmol) were each 5′-end labeled with [^{32}P]-phosphate as previously described (*22*). The polynucleotide kinase was inactivated by heating. Each labeled cross-linked duplex (50 pmol) was incubated in the presence of 5 units of T4 ligase in a buffer that contained 50 mM Tris-HCl (pH 7.5), 10 mM magnesium chloride, 100 mM sodium chloride, 10 mM dithiothreitol, 1 mM ATP, and 25 μg/mL bovine serum albumin. The ligation reactions were allowed to proceed overnight at 16 °C for **XL3** and **XL5**, whereas **XL2** was incubated for 15−60 min at 16 °C.

A 2 μL aliquot of each ligation reaction mixture was added to an equal volume of 80% glycerol containing bromophenol blue and xylene cyanol tracking dyes and loaded directly onto a 12% nondenaturing polyacrylamide gel (20 cm × 40 cm × 0.75 cm). The gel was run at approximately 650 V for 5 h at 4 °C until the bromophenol blue tracking dye had migrated 23 cm from the top of the gel. The wet gel was autoradiographed for 1 h at −80 °C with a double intensifying screen. The distances that the ligated oligomers migrated were determined and compared to the migration distances of oligomers produced by ligation of the self-complementary oligomer **M1** [d-CGGGATCCCG] and the duplex **M2** [d-GGGCAAAAAACGGCAAAAAAC/d-CCGTTTTTTGCCGTTTTTTGC] as described by Koo and Crothers (*28*).

Digestion with Restriction Enzymes. Cross-linked duplexes **XL3** and **XL5** and their non-cross-linked parents were 5′-

end labeled with [^{32}P]-phosphate as previously described (*22*). Duplex **XL3** and its parent were each dissolved in 9 μL of a solution containing 5 mM potassium acetate, 2 mM Tris-acetate, 1 mM magnesium acetate, 0.1 mM dithiothreitol, and 10 μg of bovine serum albumin (pH 7.9). The solution was heated at 100 °C for 5 min and cooled slowly to room temperature, and 1 μL (3 units) of *Acl*I was added. Duplex **XL5** and its parent were each dissolved in 9 μL of a solution containing 5 mM sodium chloride, 1 mM Tris-hydrochloride, 1 mM magnesium chloride, and 0.1 mM dithiothreitol (pH 7.9). The solution was heated at 100 °C for 5 min and cooled slowly to room temperature, and 1 μL (20 units) of *Hin*dIII was added. Each of the reaction mixtures was then divided into four aliquots (2.5 μL) which were incubated for 4 h at 16 °C, overnight at 16 °C, for 4 h at 37 °C, or overnight at 37 °C. The products of each reaction were analyzed by PAGE on a 20% gel run under denaturing conditions.

RESULTS

Syntheses of Cross-Linked Duplexes. The structure of the N^{4}C−ethyl−N^{4}C cross-link and the sequences of the duplexes containing the cross-link are shown in Figure 1. Duplexes were prepared that contain several different orientations of the N^{4}C−ethyl−N^{4}C cross-link. The cross-linked Cs in duplexes **XL1** and **XL2** are directly opposite each other and thus constitute a C−C mismatch. Examination of molecular models suggests that the ethyl linker is sufficiently long to span the distance between the C exocyclic amino groups with minimal distortion of the DNA helix. This C−C cross-link approximates the structure of the interstrand N^{3}C−ethyl−N^{1}G cross-link formed when a C−G base pair reacts with BCNU (*19*) and the recently reported N^{3}C−ethyl−N^{3}C cross-link formed by the reaction of a C−C mismatched base pair with mechloroethamine (*23*, *24*). Duplex **XL1** contains 10 base pairs plus the C−C cross-link, whereas **XL2** contains seven base pairs and three unpaired bases at the 3′-end of each strand. These duplexes are similar to previously reported C−C cross-linked duplexes that contain 5′-overhanging ends.

Duplexes **XL3** and **XL4** each contain a "staggered" N^{4}C−ethyl−N^{4}C cross-link that connects the C residues on opposite strands of the −CG− sequence. Although the distance between the exocyclic amino groups of the two C residues (4.22 Å) is somewhat greater than that between mismatched C residues (3.88 Å), molecular models suggest that the ethyl linker can span this distance without seriously distorting the helix. Duplex **XL3** contains eight base pairs and two unpaired bases at the 3′-end of each strand. Duplex **XL4** contains 12 base pairs and four unpaired C residues at the 5′-end of each strand.

Like **XL3** and **XL4**, duplexes **XL5** and **XL6** also contain a staggered N^{4}C−ethyl−N^{4}C cross-link. However, this cross-link connects the C residues on opposite strands of a −GC− sequence. Because the distance between the C residues in the B-form is ∼5.65 Å, the presence of this cross-link would be expected to introduce significant distortions into this duplex. Duplex **XL5** contains eight base pairs and a two-base 3′-overhang, whereas duplex **XL6** contains 12 base pairs and a four-base 5′-overhang.

The cross-linked duplexes were synthesized using the protected N^{4}C−ethyl−N^{4}C cross-link phosphoramidite **1.8**. This reagent was prepared as shown in Scheme 1. 5′-*O*-(Dimethoxytrityl)-2′-deoxyuridine (**1.1**) was converted to either the *O*^{4}-triazolyl-3′-*O*-*tert*-butyldimethylsilyl (**1.3**) or *O*^{4}-triazolyl-3′-*O*-trimethylsilyl (**1.5**) derivative. Treatment of **1.5** with ethylenediamine resulted in removal of the trimethylsilyl group and displacement of the triazole moiety to give *N*^{4}-(2-aminoethyl)-5′-*O*-(dimethoxytrityl)-2′-deoxycytidine (**1.6**). Reaction of **1.6** with **1.3** gave the protected N^{4}C−ethyl−N^{4}C cross-link (**1.7**) which was converted to its 3′-*O*-(*β*-cyanoethyl-*N*,*N*′-diisopropyl)phosphoramidite derivative (**1.8**).

The cross-linked duplexes were synthesized as shown in Scheme 2. One arm of the duplex was first synthesized on a controlled pore glass support, and N^{4}C−ethyl−N^{4}C cross-link phosphoramidite **1.8** was used to introduce the cross-link at the 5′-end of the oligomer to give **2.1**. The dimethoxytrityl groups were removed by brief treatment with 2% dichloroacetic acid in methylene chloride. The upper and lower strands of the duplex were extended in the 5′-direction simultaneously by repetitive coupling with protected nucleoside 3′-phosphoramidites to give the branched Y-intermediate, **2.2a**. Following addition of the last nucleotide, the dimethoxytrityl groups of **2.2a** were removed and the 5′-hydroxyl groups were "capped" by reaction with acetic anhydride to give the acetylated Y-intermediate, **2.2b**.

The *tert*-butyldimethylsilyl (TBDMS) group was then removed from **2.2b** by treating the support with anhydrous tetra-*n*-butylammonium fluoride (TBAF) in tetrahydrofuran. Because fluoride-mediated desilylation can result in cleavage of adjacent *β*-cyanoethylphosphotriester linkages (*22*), the protected oligomer was first treated with anhydrous triethylamine to convert the triester groups to phosphodiester linkages. A similar strategy was used previously in the synthesis of branched oligoribonucleotides (*29*, *30*). The efficiency of removing the TBDMS group appeared to depend on the structure of the Y-intermediate. For example, 70% desilylation of the Y-intermediate of **XL2** was observed after TBAF treatment for 10 min, whereas 45% desilylation of the Y intermediate of **XL1** was observed after 20 min.

The complete duplex, **2.3**, was prepared by repetitive coupling of the 3′-end of the Y-intermediate with protected nucleoside 5′-phosphoramidites. To maximize these coupling yields, the phosphoramidites were used at a concentration of 0.3 M instead of the usual concentration (0.15 M) used for nucleoside 3′-phosphoramidites. In addition, it was found to be necessary to increase the total detritylation time to 120 s to effect complete removal of the 3′-*O*-dimethoxytrityl groups.

The cross-linked oligomers were deprotected by treating the support with concentrated ammonium hydroxide at 65 °C. The duplexes were purified by strong anion exchange HPLC using a sodium chloride gradient in buffer that contained 100 mM Tris-HCl and 10% acetonitrile. The duplexes, whose retention times are shown in Table 1, eluted as single peaks and were obtained in varying yields. Duplex **XL2**, which was obtained in the lowest yield, was particularly difficult to purify by HPLC due most likely to three 3′-overhanging G residues. The major side product in these syntheses, the deprotected form of **2.2b**, resulted from incomplete desilylation of the TBS-protected Y-intermediate.

Samples of each duplex were digested with a combination of snake venom phosphodiesterase and calf intestinal phos-

Scheme 1

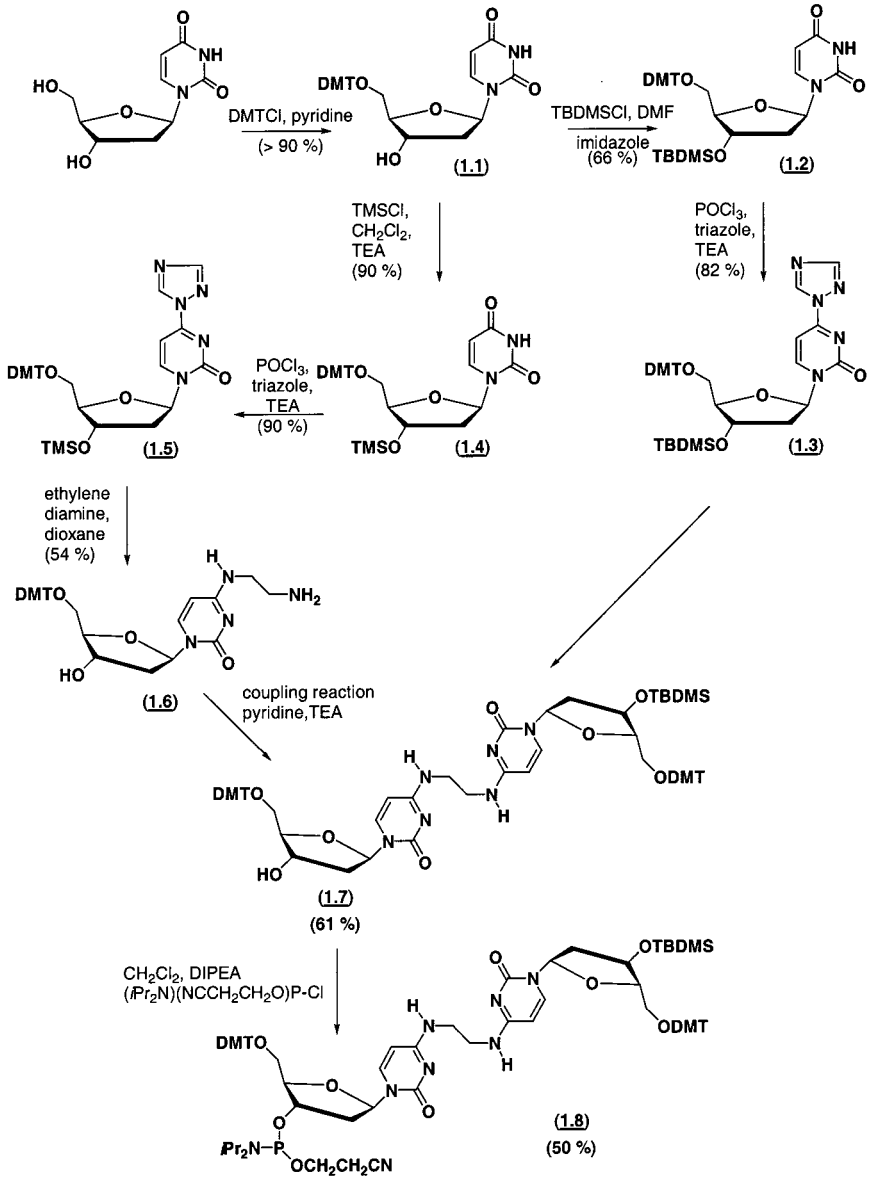

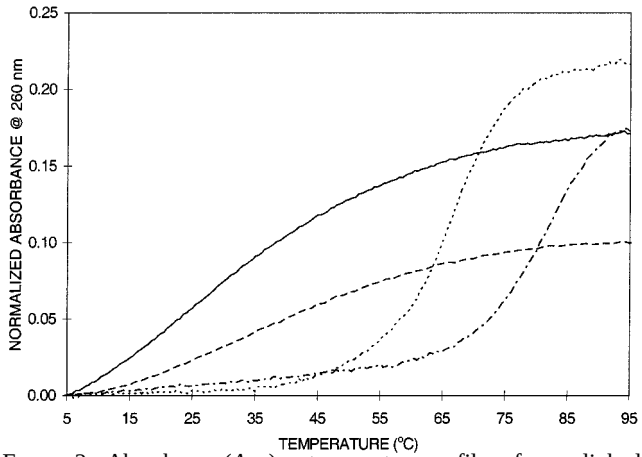

FIGURE 2: Absorbance (A_{260}) vs temperature profiles of cross-linked duplexes **XL1** (···), **XL2** (− − −), **XL3** (−·−), and **XL5** (—). Solutions containing 1 μM duplex in 90 mM sodium chloride, 10 mM sodium phosphate, and 1 mM ethylenediaminetetraacetate buffer (pH 7.0) were heated at 0.5 °C/min.

phatase, and the digests were analyzed by C-18 reversed phase HPLC. As shown in Table 1, each duplex was hydrolyzed to its component nucleosides and the N⁴C−ethyl−N⁴C cross-link in ratios consistent with the structure of the particular duplex. In addition to this characterization, the molecular weight of each duplex, as determined by MALDI TOF mass spectrometry, was consistent with the structure of the duplex. These data are also shown in Table 1.

Thermal Denaturation. Ultraviolet thermal denaturation experiments were carried out to assess the effects of the various cross-links on duplex stability. Denaturation curves for cross-linked duplexes **XL1**−**XL3** and **XL5** are shown in Figure 2. Duplexes **XL1** and **XL2**, which contain cross-linked C−C mismatches, both have sigmoidal denaturation profiles. The midpoint of the transition curve (T_m) of **XL2**, which in addition to the C−C cross-link has six A−T base pairs, is 32 °C. This value is similar to that observed previously, 29 °C, for the duplex d(AAAC*TTTCCCC)$_2$ where C* is a C−C cross-link (*22*). Duplex **XL1** on the other hand has a much higher T_m (65 °C). Furthermore, the denaturation curve of **XL1** is much sharper and displays approximately twice the hyperchromicity of that of duplex

Scheme 2

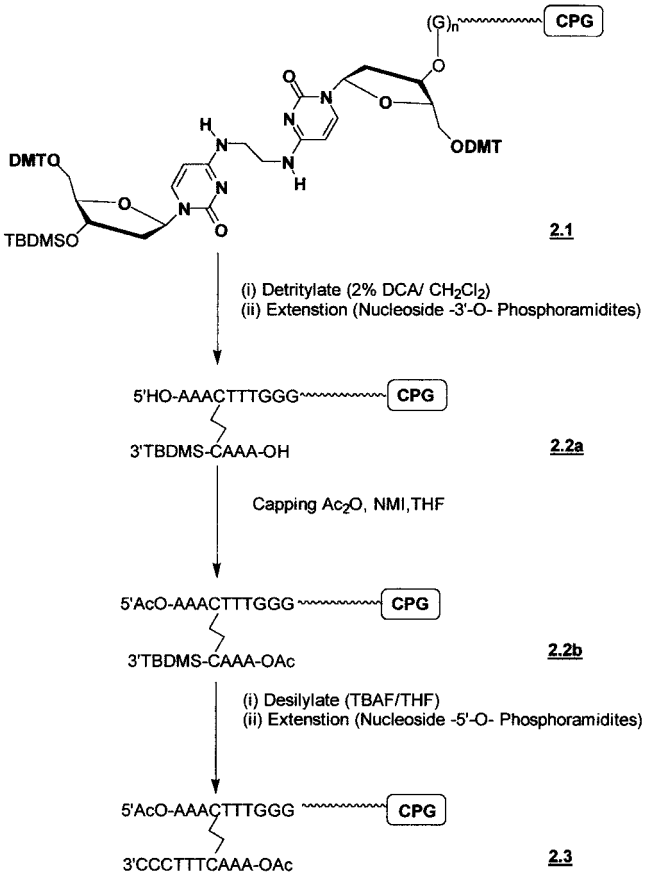

Table 2: Thermal Denaturation of Cross-Linked Duplexes and Their Non-Cross-Linked Controls

	T_m (°C)[a]			T_m (°C)[a]	
duplex	control[b]	cross-link	duplex	control[b]	cross-link
XL1	40 (27)[c]	65	**XL3**	32	81
XL2	<5 (<0)[c]	32	**XL5**	30	20

[a] Experiments were carried out in buffer containing 90 mM sodium chloride, 10 mM sodium phosphate, and 1 mM ethylenediaminetetraacetate buffer (pH 7.0). The concentration of each strand was 2 μM. [b] Duplexes in which G−C base pairs replace the cross-link. [c] Duplex in which a C−C mismatch replaces the cross-link.

XL2. As shown in Table 2, the transition temperatures of both **XL1** and **XL2** are approximately 25 °C higher than the melting temperatures of the corresponding non-cross-linked duplexes, which have a C−G base pair in place of the N^4C−ethyl−N^4C cross-link.

Duplex **XL3**, which contains a −CG− staggered cross-link, has a very sharp thermal denaturation curve with a remarkably high transition temperature (81 °C). In contrast to this behavior, duplex **XL5**, which contains a −GC− staggered cross-link, has very low thermal stability. As seen in Figure 2, the transition curve, the midpoint of which is 20 °C, is very broad, although the overall hyperchromicity of this duplex is the same as that of **XL3**. Despite the presence of a covalent cross-link, the thermal stability of **XL5** is lower than that of its non-cross-linked parent, the T_m of which is 30 °C.

The unusually high thermal stability of **XL3** is reflected by its behavior on a denaturing polyacrylamide gel. As shown in Figure 3, cross-linked duplexes **XL2** and **XL5**, which

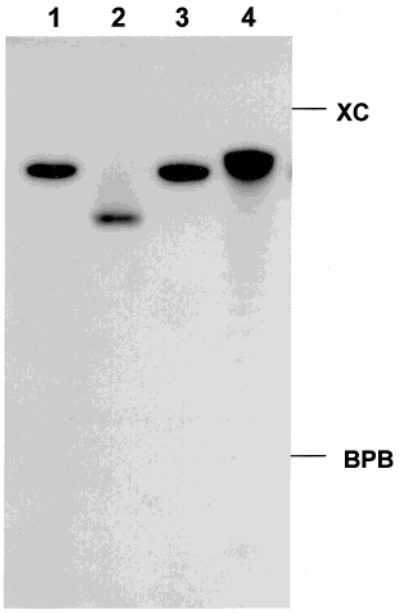

FIGURE 3: Polyacrylamide gel electrophoresis of cross-linked duplexes. Cross-linked duplexes **XL2** (lane 1), **XL3** (lane 2), and **XL5** (lane 3) and a control oligomer, d(T_{22}) (lane 4), were each 5′-end labeled with [γ-^{32}P]ATP and subjected to electrophoresis on a 20% polyacrylamide gel run under denaturing conditions. XC and BPB are xylene cyanol and bromophenol blue dyes, respectively.

consist of 20 nucleotides, each have approximately the same electrophoretic mobility as that of d(T_{22}). In contrast, cross-linked duplex **XL3** has a significantly faster mobility on the gel. Similar behavior was observed when **XL4** and **XL6** were subjected to electrophoresis under the same conditions. Thus, **XL4**, which contains a −CG− staggered cross-link, migrates more rapidly than **XL6** (data not shown).

Circular Dichroism Spectra. Circular dichroism (CD) spectra of cross-linked duplexes **XL1**, **XL3**, and **XL5** and their non-cross-linked parents were recorded at 5 °C in the same buffer that was used for the thermal denaturation studies. Under these conditions, both the cross-linked and non-cross-linked oligomers should be in their base-paired, duplex form. Both **XL1** and the non-cross-linked version of this duplex have very similar CD spectra as shown in Figure 4A. The C−C cross-linked duplex has maxima at 278 and 218 nm and a minimum at 250 nm. The spectrum of the parent duplex is shifted to a slightly longer wavelength and has a smaller positive and negative molar ellipticity. Overall, the spectra of both duplexes are similar to that of canonical B-form DNA (*31*).

The CD spectrum of duplex **XL3**, which contains a −CG− staggered cross-link, is distinctly different from that of **XL1** as shown in Figure 4B. The spectrum contains two maxima at 276 and 222 nm and two minima at 298 and 253 nm. Although the parent duplex has maxima at 280 and 221 nm and a minimum at 249 nm, it lacks the negative peak at 298 nm seen in the cross-linked duplex. In addition, the molar ellipticity of **XL3** at 276 nm is approximately 66% of that of the non-cross-linked parent at the same wavelength.

Duplex **XL5**, which contains a −GC− staggered cross-link, is qualitatively similar to that of **XL1** and to its non-cross-linked parent as shown in Figure 4C. However, in this case, the cross-linked duplex has a greater molar ellipticity at 278 and 210 nm than the non-cross-linked duplex.

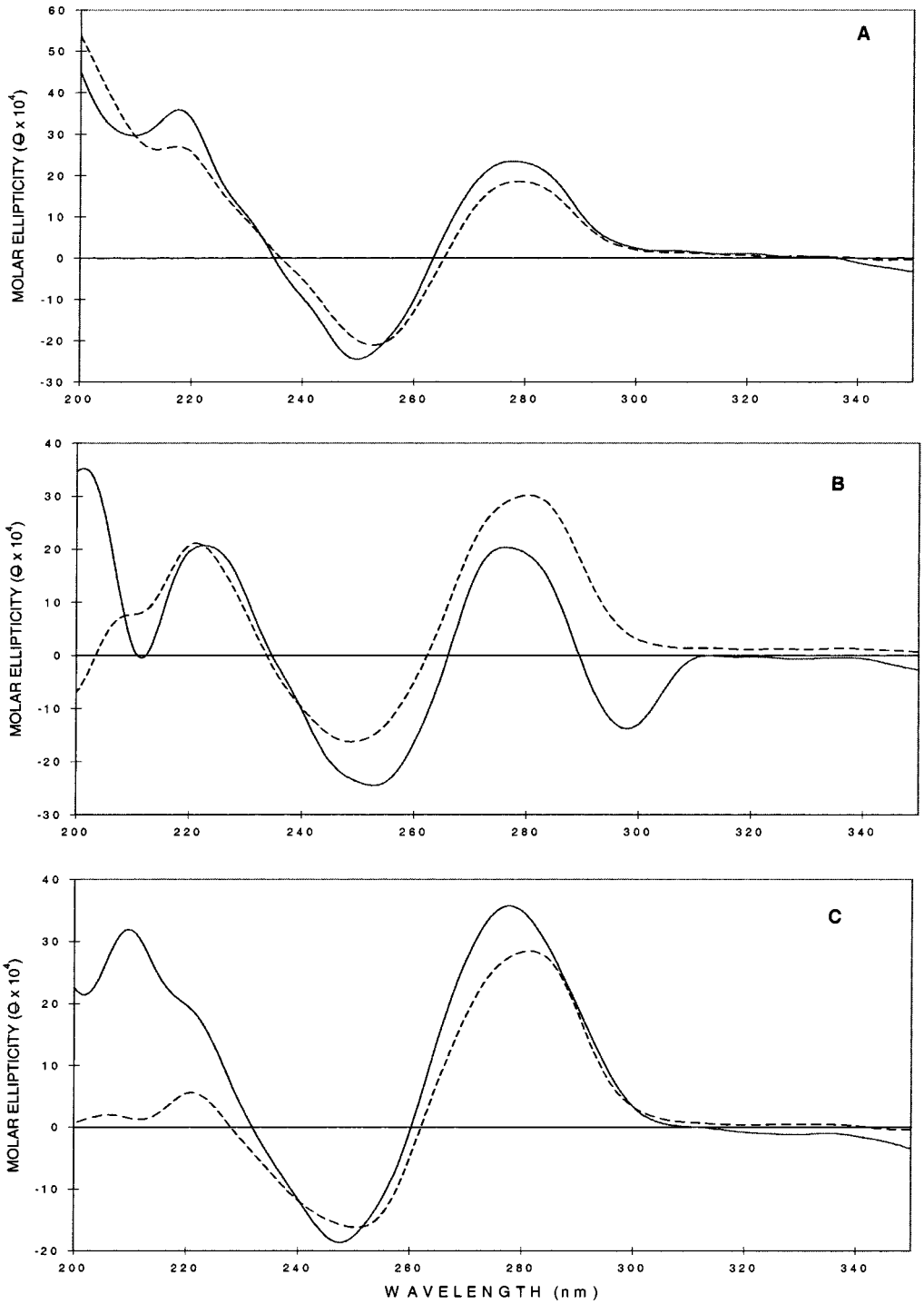

FIGURE 4: Circular dichroism spectra of (A) cross-linked duplex **XL1** (—) and its non-cross-linked parent (– – –), (B) cross-linked duplex **XL3** (—) and its non-cross-linked parent (– – –), and (C) cross-linked duplex **XL5** (—) and its non-cross-linked parent (– – –). Spectra were recorded at 5 °C in a buffer containing 90 mM sodium chloride 10 mM sodium phosphate, and 1 mM ethylenediaminetetraacetate buffer (pH 7.0).

Self-Ligation Experiments. Duplexes **XL2**, **XL3**, and **XL5** have complementary, 3′-overhanging ends and can potentially undergo self-ligation. The duplexes were phosphorylated with polynucleotide kinase, and the phosphorylated duplexes were incubated with T4 DNA ligase in the presence of ATP. The reaction mixtures were then analyzed on nondenaturing polyacrylamide gels as shown in Figure 5. Two additional duplexes, **M-1**, a self-complementary 10-mer, and **M-2**, a 21-mer that contains a six base-pair A−T tract (*28*), were also self-ligated and served as size markers on the gel.

Duplex **XL2** underwent rapid self-ligation. As shown in lane 2 of Figure 5A, a ladder of multimeric products was observed after incubation for 15 min at 16 °C. Incubation overnight resulted in the formation of high-molecular weight products as shown in lane 3 of Figure 5B.

Duplex **XL3** also underwent self-ligation, as shown by the ladder in lane 4 of Figure 5B. The reaction appeared to proceed at a slower rate than the **XL2** reaction, and no high-molecular weight circular products were observed even after overnight incubation. As shown in lane 5 of Figure 5B, essentially no multimeric products were observed when

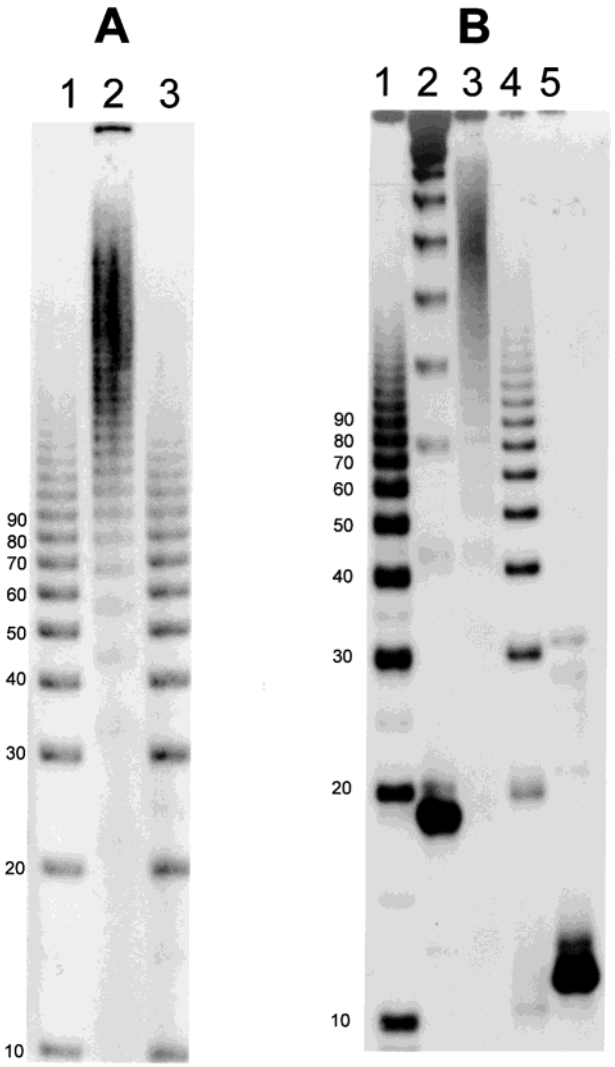

FIGURE 5: Self-ligation of cross-linked duplexes. 5′-Phosphorylated cross-linked duplexes and non-cross-linked control duplexes were ligated at 16 °C in the presence of T4 DNA ligase as described in Experimental Procedures and the reaction mixtures subjected to electrophoresis on a 20% polyacrylamide gel run under non-denaturing conditions. Panel A shows the ligation products of non-cross-linked duplex **M1** (lanes 1 and 3) and cross-linked duplex **XL2** (lane 2). Panel B shows the ligation products of non-cross-lined duplex **M1** (lane 1), A-tract duplex **M2** (lane 2), and cross-linked duplexes **XL2** (lane 3), **XL3** (lane 4), and **XL5** (lane 5). Duplex **XL3** was ligated for 15 min (A**)** or overnight (B), whereas **XL2** and **XL3** were each ligated overnight. Oligomer **M1** is d(CGGGATCCCG), and duplex **M2** is d(GGGCAAAAAACG-GCAAAAAAC)/d(CCGTTTTTTGCCGTTTTTTGC).

duplex **XL5** was incubated with T4 DNA ligase and ATP.

The relative lengths, R_L, of the ligation products of duplexes **XL2** and **XL3** were determined by comparing their electrophoretic mobilities to those of oligomers formed by ligation of duplex **M-1** (*28*, *32*). Ligation of duplex **M-1** produces a series of oligonucleotides that differ by multiples of 10 base pairs as shown in lanes 1 and 3 of panel A and lane 1 of panel B of Figure 5. The relative lengths were plotted against the actual chain length of the oligomers produced by ligation. As shown in Figure 6, ligation products from both **XL2** and **XL3** gave essentially linear plots with only a slight deviation from an R_L of 1.00 over the chain length range of 20−150 base pairs. In contrast to this behavior, a similar plot of R_L versus the chain length of the

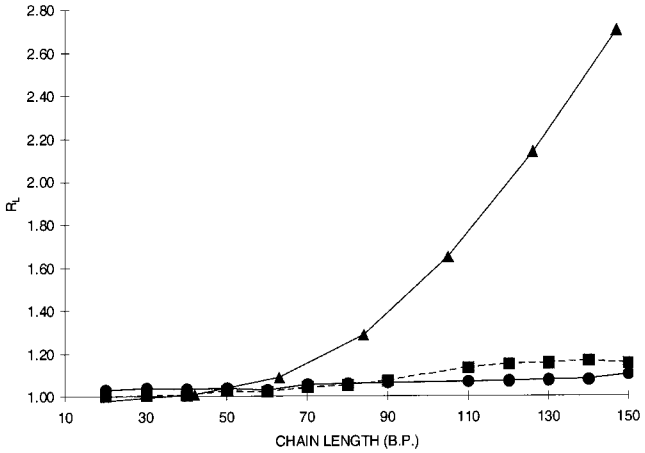

FIGURE 6: Relative chain lengths (R_L) vs actual chain lengths of cross-linked duplexes **XL2** (■) and **XL3** (●), and of non-cross-linked duplex **M2** (▲), which contains an A tract. R_L was determined as the ratio of the migration distance of an **M1** oligomer of chain length *n* to the migration distance of the oligomer of the cross-linked duplex of chain length *n*.

ligation products of duplex **M-2**, the ligation ladder of which is shown in lane 2 of Figure 5B, exhibited a strong positive deviation from $R_L = 1.00$ as the chain length of the oligomers increased. This deviation is consistent with bending induced by the presence of the six-base A tract in duplex **M-2** (*28*).

DISCUSSION

We previously described the syntheses of C−C cross-linked duplexes similar in structure to that of **XL1** (*22*). These were prepared using a convertible nucleoside approach which transforms an O^4-triazoylyldeoxyuridine residue located on the first 3′-arm of the nascent, support-bound duplex to the C−C cross-link. The cross-linked duplexes shown in Figure 1 were prepared by an alternative procedure that uses the protected N^4C−ethyl−N^4C cross-link phosphoramidite, **1.8**, to introduce the cross-link directly during the synthesis of the duplex. This phosphoramidite is easily synthesized from readily available components and provides a convenient reagent for the construction of a variety of cross-linked duplexes having either blunt or 5′- or 3′-overhanging ends.

The two dimethoxytrityl groups located on the 5′-hydroxyls of the cross-link can be removed in the presence of the 3′-*tert*-butyldimethylsilyl group. This selective deprotection allows simultaneous synthesis of the two 5′-arms of the duplex to give a Y-shaped intermediate that terminates its 3′-end with the TBDMS group. The 5′-dimethoxytrityl groups on each of the 5′-arms of the Y-intermediate were removed and replaced with 5′-acetyl groups before synthesis of the duplex was continued.

Removal of the TBDMS group by treatment of the Y-intermediate with TBAF resulted in variable yields of desilylation with the different oligomers. This variation appears to be a function of the number of nucleotides surrounding the cross-link. Thus, the Y-intermediate of **XL2** contains three 5′-nucleotides (AAA) on each branch of the cross-link. On the other hand, the Y-intermediate of **XL1** contains five 5′-nucleotides (GCAAA) on each branch of the cross-link. The increased charge density in the backbone of **XL1** compared to that in **XL2** could result in stronger charge repulsion between the oligomer and the negatively

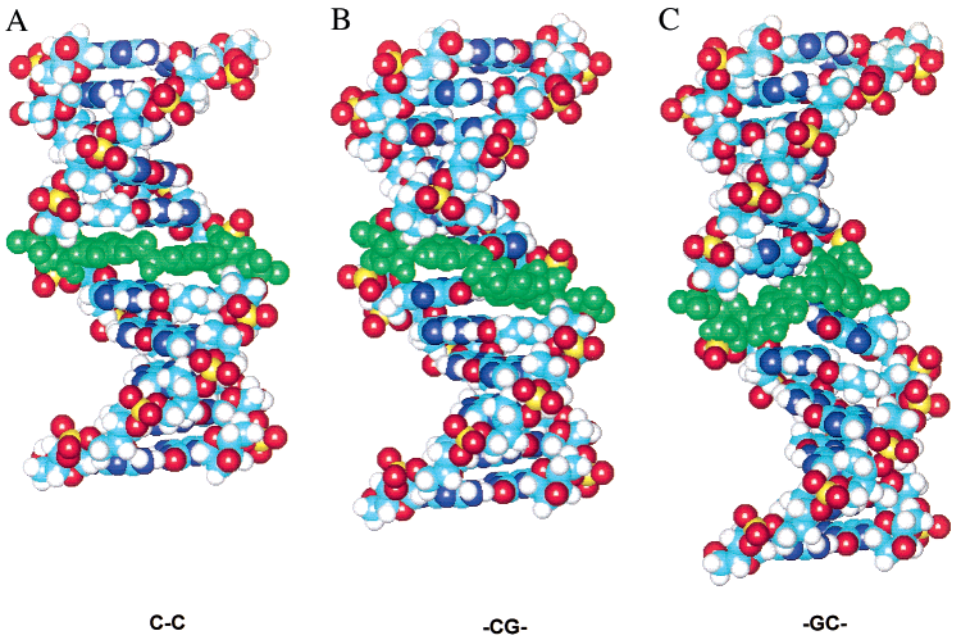

FIGURE 7: Molecular models of a self-complementary duplex, d[(CCAGTCACTCC)$_2$], that contains a mismatched C−C, a C−G staggered, or a G−C N⁴C−ethyl−N⁴C cross-link (shown in green). The models were built using Hyper Chem molecular modeling software and energy minimized using the Amber force field.

charged fluoride ion and thus account for the reduced level of desilylation. Steric factors may also play a role in incomplete desilylation. Thus, prolonged treatment with TBAF did not significantly increase the amount of desilylation, suggesting that some portion of the TBDMS groups on the support-bound oligomer are not accessible to the reagent. It may be possible to improve overall yields by choosing a different 3′-protecting group. Thus, the allyloxycarbonyl group has been used to protect the 3′-OH group during the synthesis of a nitrous acid cross-linked DNA duplex (*21*) and a DNA duplex containing a covalently cross-linked base pair (*33*). Despite the variable yields resulting from incomplete desilylation, our procedure provided sufficient quantities of cross-linked oligomers for physical and biological studies.

Duplexes **XL1** and **XL2** contain an ethyl cross-link between two mismatched C residues on opposite strands of the duplex. Examination of the molecular model shown in Figure 7A suggests that the ethyl cross-link should be accommodated in the major groove of the duplex with minimal distortion of the helix and minimal steric interaction with its neighboring A−T base pairs. The shapes of the UV thermal denaturation profiles of these cross-linked oligomers suggest that both exist as duplexes and that the base pairs surrounding the cross-link melt in a cooperative manner (see Figure 2). The difference in the transition temperatures between **XL1** and **XL2** (33 °C) is similar to the difference in T_m between the corresponding duplexes in which the C−C cross-links are replaced with G−C base pairs. Thus, the higher stability of **XL1** versus that of **XL2** most likely reflects the presence of four additional G−C base pairs in the former duplex. Replacement of the C−C cross-link in **XL1** with a C−C mismatch results in a dramatic reduction in the T_m, consistent with the destabilizing effect of C−C mismatches (*34*). Similar substitution in **XL2** results in complete loss of duplex formation.

The transition temperatures of **XL1** and **XL2** are at least 25 °C higher than the melting temperatures of control duplexes in which the cross-link is replaced with a G−C base pair. Similar enhancements in stability have been observed in duplexes that contain a terminal disulfide cross-link (*35*) or a covalently linked base pair (*36*), and in duplexes that contain internal psoralen (*37*) or mitomycin C (*14*) interstrand cross-links. The most likely reasons for this increased stability are the reduction in molecularity and the reduction in entropy that result from the presence of the cross-link (*35*).

The CD spectrum of **XL1** shows that this duplex is in a B-conformation (see Figure 4). The close similarity of this spectrum to that of the non-cross-linked parent again suggests that the cross-link does not significantly perturb the overall structure of the helix. Further evidence for this is found in the ligation experiment. Duplex **XL2** has self-complementary 3′-overhanging ends that enable it to undergo self-ligation. Such ligation produces a series of oligonucleotides each differing in length by 10 base pairs where the C−C cross-links are in phase with the periodicity of the helix. Distortion or bending caused by the cross-link could thus be detected by anomalous mobility on a nondenaturing polyacrylamide gel (*32*). As shown in Figure 6, there was essentially no deviation of the relative chain length, R_L, as a function of oligomer chain length from a value of 1.00. This result suggests that the C−C cross-link does not bend the helix to any significant extent.

Duplexes **XL3** and **XL4** each contain a "staggered" ethyl cross-link that connects the two C residues of a central −CG− step in the duplex. Although the distance between the N⁴C exocylic amino groups is somewhat greater than in the case of the C−C cross-linked duplexes, the molecular model suggests (see Figure 7B) that the cross-link is sufficiently long to span this distance with minimal perturbation of the helix. The model also suggests that slight propeller twisting of the cross-linked −CG− base sequence would allow hydrogen bond contacts to be maintained between the C−G base pairs. In fact, the presence of the −CG− staggered cross-link produces an extremely stable duplex. The transition

temperature of this duplex (81 °C) is 49 °C higher than the melting temperature of the corresponding non-cross-linked duplex, a result that suggests the staggered cross-link provides even greater stabilization of adjacent base pairs than does the C−C cross-link. Consistent with this suggestion is the observation that the transition temperature of **XL3** is 49 °C higher than that of **XL2**, although **XL3** contains only one more base pair than **XL2**. Furthermore, the transition temperature of **XL3**, which contains four G−C and four A−T base pairs, is 16 °C higher than that of **XL1**, which in addition to the cross-link has four G−C and six A−T base pairs.

The extraordinary stability of **XL3** is also seen when the duplex is electrophoresed under denaturing conditions on a polyacrylamide gel. Duplexes **XL2** and **XL5**, each of which contains 20 nucleotides, migrate in a manner similar to that of d-T_{22}. Thus, the cross-linked duplexes behave essentially as single-stranded oligonucleotides under the denaturing conditions of the gel. Duplex **XL3** on the other hand migrates more rapidly through the gel. This behavior suggests that despite the denaturing conditions, **XL3** continues to migrate like a base-paired or partially base-paired duplex. Similar differences in migration were seen between **XL4** and **XL6,** suggesting that duplex stabilization by the −CG− staggered cross-link is not unique to shorter duplexes such as **XL3**.

Unlike that of duplex **XL1**, the CD spectrum of **XL3** differs from that of B-form DNA. This difference, which takes the form of a negative band at 298 nm, is not seen in the non-cross-linked parent duplex, the spectrum of which is similar to that of the non-cross-linked parent of **XL1**. The negative band may arise from a local conformational change in the helix, possibly due to propeller twisting of the cross-linked base pairs. Further insight into this perturbation awaits a more detailed analysis of **XL3** by NMR spectroscropy.

Although the −CG− staggered cross-link appears to perturb the structure of the helix, this perturbation is not of sufficient magnitude to be detected by gel electrophoresis. Thus, the R_L values of oligomers resulting from self-ligation of **XL3** do not deviate significantly from unity over a chain length range of 20−150 base pairs.

Duplexes **XL5** and **XL6** each contain a −GC− staggered cross-link. The distance between the two N^4C exocyclic amino groups in this sequence is 5.65 Å in the B-form helix which is greater than the length of the ethyl linker. Consequently, this cross-link would be expected to disrupt G−C base pairing at the cross-link site. The resulting distortion could also affect the adjacent A−T base pairs as shown by the molecular model in Figure 7C.

Not surprisingly, the −GC− staggered cross-link in **XL5** destabilizes the duplex. The melting transition of **XL5** is 20 °C, which is 10 °C lower than the T_m of its parent non-cross-linked duplex. The broad shape of the denaturation curve relative to those of duplexes **XL1** and **XL3** suggests reduced cooperativity. At ambient temperature, **XL5** most likely exists in a partially denatured form. Despite the destabilizing effect of the cross-link, the overall structure of the cross-linked duplex at 5 °C appears to be similar to that of the non-cross-linked parent duplex and B-DNA as monitored by CD spectroscopy.

Attempts to self-ligate **XL5** at 16 °C were not successful. This may be due to the partially denatured state of the duplex at this temperature. However, we have found that duplex **XL6**, which contains four additional G−C base pairs, is readily ligated into plasmid DNA.

Duplexes **XL4** and **XL6** contain recognition sites for *Acl*I and *Hin*dIII restriction endonucleases, respectively. Although both non-cross-linked parent duplexes were completely cleaved after 4 h when incubated with their cognate endonuclease at 16 °C, **XL4** and **XL6** were totally resistant, even after incubation for 2 days (data not shown). The presence of the ethyl cross-link in the major groove of each duplex most likely accounts for this lack of reactivity. Previous studies on a Dickerson dodecamer that contains disulfide cross-links at either end of the duplex showed that the cross-linked duplex is completely cleaved by *Eco*RI endonuclease (*35*).

CONCLUSIONS

Cross-link phosphoramidite **1.8** is a convenient reagent that can be used to place an N^4C−ethyl−N^4C cross-link at a specific site in a DNA duplex. The synthetic procedure provides sufficient material for a variety of physical and biological studies. Duplexes with uniquely oriented cross-links can be prepared by altering the order of addition of the bases surrounding the cross-link. The relative orientation of the cross-link gives rise to duplexes of different structures and stabilities. In preliminary experiments, we have found that plasmid DNA containing these cross-linked duplexes can be repaired in *Escherichia coli.* The results of these repair studies will be reported in due course.

NOTE ADDED IN PROOF

Modifications were made to the name of compound **1.6**, oligomer **M1**, and duplex **M2**, and Scheme 2 was replaced.

REFERENCES

1. Thomas, C. B., Osieka, R., and Kohn, K. W. (1978) *Cancer Res. 38*, 2448−2453.
2. Erickson, L. C., Bradley, M. O., Ducore, J. M., Ewig, R. A. G., and Kohn, K. W. (1980) *Proc. Natl. Acad. Sci. U.S.A. 77*, 467−471.
3. Garcia, S. T., McQuillan, A., and Panasci, L. (1988) *Biochem. Pharmacol. 37*, 3189−3192.
4. Colvin, M. (1982) *The Alkylating Agents*, W. B. Saunders Co., Philadelphia.
5. Friedberg, E. C., Walker, G. C., and Siede, W. (1995) *DNA Repair and Mutagenesis*, ASM Press, Washington, DC.
6. Ojwang, J. O., Grueneberg, D. A., and Loechler, E. L. (1989) *Cancer Res. 49*, 6529−6537.
7. Grueneberg, D. A., Ojwang, J. O., Benasutti, M., Hartman, S., and Loechler, E. L. (1991) *Cancer Res. 51*, 2268−2272.
8. Rink, S. M., Solomon, M. S., Taylor, M. J., Rajur, S. B., McLaughlin, L. W., and Hopkins, P. B. (1993) *J. Am. Chem. Soc. 115*, 2551−2557.
9. Rink, S. M., and Hopkins, P. B. (1995) *Biochemistry 34*, 1439−1445.
10. Van Houten, B., Gamper, H., Hearst, J. E., and Sancar, A. (1986) *J. Biol. Chem. 261*, 14135−14141.
11. Huang, H., Woo, J., Alley, S. C., and Hopkins, P. B. (1995) *Bioorg. Med. Chem. 3*, 659−669.
12. Paquet, F., Boudvillain, M., Lancelot, G., and Leng, M. (1999) *Nucleic Acids Res. 27*, 4261−4268.
13. Millard, J. T., Weidner, M. F., Kirchner, J. J., Ribeiro, S., and Hopkins, P. B. (1991) *Nucleic Acids Res. 19*, 1885−1891.
14. Warren, A. J., and Hamilton, J. W. (1996) *Chem. Res. Toxicol. 9*, 1063−1071.
15. Kirchner, J. J., Sigurdsson, S. T., and Hopkins, P. B. (1992) *J. Am. Chem. Soc. 114*, 4021−4027.

16. Huang, H., and Hopkins, P. B. (1993) *J. Am. Chem. Soc. 115*, 9402−9408.
17. Alley, S. C., Brameld, K. A., and Hopkins, P. B. (1994) *J. Am. Chem. Soc. 116*, 2734−2741.
18. Tsarouhtsis, D., Kuchimanchi, S., Decorte, B. L., Harris, C. M., and Harris, T. M. (1995) *J. Am. Chem. Soc. 117*, 11013−11014.
19. Fischhaber, P. L., Gall, A. S., Duncan, J. A., and Hopkins, P. B. (1999) *Cancer Res. 59*, 4363−4368.
20. Dooley, P. A., Tsarouhtsis, D., Korbel, G. A., Nechev, L. V., Shearer, J., Zegar, I. S., Harris, C. M., Stone, M. P., and Harris, T. M. (2001) *J. Am. Chem. Soc. 123*, 1730−1739.
21. Harwood, E. A., Sigurdsson, S. T., Edfeldt, N. B. F., Reid, B. R., and Hopkins, P. B. (1999) *J. Am. Chem. Soc. 121*, 5081−5082.
22. Noll, D. M., Noronha, A. M., and Miller, P. S. (2001) *J. Am. Chem. Soc. 123*, 3405−3411.
23. Romero, R. M., Mitas, M., and Haworth, I. S. (1999) *Biochemistry 38*, 3641−3648.
24. Romero, R. M., Rojsitthisak, P., and Haworth, I. S. (2001) *Arch. Biochem. Biophys. 386*, 143−153.
25. Beaucage, S., and Caruthers, M. H. (1981) *Tetrahedron Lett. 22*, 1859−1862.
26. Damha, M. J., Giannaris, P. A., and Zabarylo, S. V. (1990) *Nucleic Acids Res. 18*, 3813−3821.
27. Puglisi, J. D., and Tinoco, I. J. (1989) *Methods Enzymol. 180*, 304−325.
28. Koo, H.-S., and Crothers, D. M. (1988) *Proc. Natl. Acad. Sci. U.S.A. 85*, 1763−1767.
29. Kierzek, R., Kopp, D. W., Edmonds, M., and Caruthers, M. H. (1986) *Nucleic Acids Res. 14*, 4751−4764.
30. Ganeshan, K., Tady, T., Nam, K., Braich, R., Purdy, W. C., Boeke, J. D., and Damha, M. J. (1995) *Nucleosides Nucleotides 14*, 1009−1013.
31. Gray, D. M., Ratliff, R. I., and Vaughan, M. R. (1992) *Methods Enzymol. 211*, 389−405.
32. Bellon, S. F., and Lippard, S. J. (1990) *Biophys. Chem. 35*, 179−188.
33. Li, H.-Y., Qiu, Y.-L., Moyroud, E., and Kishi, Y. (2001) *Angew. Chem., Int. Ed. 40*, 1471−1475.
34. Peyret, N., Seneviratne, P. A., Allawi, H. T., and John SantaLucia, J. (1999) *Biochemistry 38*, 3468−3477.
35. Osborne, S. E., Vollker, J., Stevens, S. Y., Breslauer, K. J., and Glick, G. D. (1996) *J. Am. Chem. Soc. 118*, 11993−12003.
36. Li, H.-Y., Qiu, Y.-L., and Kishi, Y. (2001) *ChemBioChem*, 371−374.
37. Shi, Y.-b., and Hearst, J. E. (1986) *Biochemistry 25*, 5895−5902.

BI011610U